

UrQMD calculations of two-pion HBT correlations in p+p and Pb+Pb collisions at LHC energies

Qingfeng Li

School of Science, Huzhou Teachers College, Huzhou 313000, P. R. China

E-mail: liqf@hutc.zj.cn

Gunnar Gräf and Marcus Bleicher

Frankfurt Institute for Advanced Studies (FIAS), Johann Wolfgang Goethe-Universität,
Ruth-Moufang-Str. 1, D-60438 Frankfurt am Main, Germany

Abstract. Two-pion Hanbury-Brown-Twiss (HBT) correlations for p+p and central Pb+Pb collisions at the Large-Hadron-Collider (LHC) energies are investigated with the ultra-relativistic quantum molecular dynamics model combined with a correlation afterburner. The transverse momentum dependence of the Pratt-Bertsch HBT radii R_{long} , R_{out} , and R_{side} is extracted from a three-dimensional Gaussian fit to the correlator in the longitudinal co-moving system. In the p+p case, the dependence of correlations on the charged particle multiplicity and formation time is explored and the data allows to constrain the formation time in the string fragmentation to $\tau_f \leq 0.8$ fm/c. In the Pb+Pb case, it is found that R_{out} is overpredicted by nearly 50%. The LHC results are also compared to data from the STAR experiment at RHIC. For both energies we find that the calculated R_{out}/R_{side} ratio is always larger than data, indicating that the emission in the model is less explosive than observed in the data.

1. Introduction

The properties of strongly interacting matter are described by the theory of Quantum-Chromodynamics (QCD). To explore the details of QCD matter under extreme conditions, one needs to compress and heat up QCD matter to regimes present microseconds after the Big Bang. Today these conditions can only be found in the interior of neutron stars or created in heavy-ion collisions at relativistic energies. Over the last decade the experimental programs at the Super Proton Synchrotron (SPS) and at the Relativistic Heavy Ion Collider (RHIC) have provided exciting pioneering data on the equation of state (EoS), the transport properties of the matter created and its spatial distributions [1, 2, 3, 4, 5, 6, 7, 8, 9, 10]. In addition, the Large Hadron Collider (LHC) at CERN had been designed, installed, tested, and repaired in the past two decades and finally, started normal operation in the end of the year 2009. Since then, a tremendous amount of experimental data in various aspects of high energy physics has been obtained and received much attention by theoretical physicists. And, the extracted bulk properties of the high temperature fireball created in such ultra-relativistic collisions have provided unprecedented information for fundamental investigations of the phase diagram of QCD. Here we want to explore the expansion properties of the created matter by investigating the spatial shape of the fireball. Although it is known that one can not measure the emission

time pattern and/or the spatial profile of the source directly, a well-established technique, called “femtoscopy” or “HBT” (see e.g. [11] and references therein) can be employed to obtain this information. Femtoscopy has been extensively used in the heavy ion community since it provides the most direct link to the lifetime and size of nuclear reactions. The ALICE collaboration has published first results of two-pion Bose-Einstein correlations in both p-p [12] and central Pb-Pb [13] collisions at LHC energies in the beginning of the year 2011. These experimental results have attracted the research interest of several theoretical groups [13, 14, 15, 16], whose models are based on hydrodynamic/hydrokinetic and hadronic microscopic approaches.

It is often argued that the particle emitting system in p+p collisions is too small to create a medium that exhibits bulk properties, this is different at a center of mass energy of $\sqrt{s}=7$ TeV. Here, the particle multiplicity is about the same as in nucleus-nucleus collisions, studied at RHIC. These data suggest that space momentum correlations are developed even in p+p collisions as soon as high particle multiplicities are achieved. Thus it is worthwhile studying the dependence of HBT observables on the event multiplicity. As the system created in p+p collisions is still small, an essential quantity that influences the particle freezeout radii is the formation time in flux tube fragmentation. The formation time sets the scale for a minimum value of the source lifetime - of course followed by resonance decay and rescattering. In this paper we suggest that the recent LHC data on p+p collisions allow us to determine the formation time in the flux tube break-up.

In this paper we show results for the HBT radii of two-pion correlations from p+p and central ($< 5\%$ of the total cross section σ_T) Pb+Pb collisions at LHC energies $\sqrt{s_{NN}} = 7$ and 2.76 TeV, respectively, from the ultra-relativistic quantum molecular dynamics (UrQMD) model [17, 18, 19, 20]. The calculations are compared to ALICE data as well as to those at the RHIC energy $\sqrt{s_{NN}} = 200$ GeV.

The paper is arranged as follows: In Section 2, a brief description of the UrQMD model and the treatment of the HBT correlations as well as the corresponding Gaussian fitting procedure are shown. Section 3 gives the main results of the model calculations for p+p and Pb+Pb collisions at LHC energies. Finally, in Section 4, a summary is given.

2. Brief description of the UrQMD model and the HBT Gaussian fitting procedure

UrQMD [19, 20, 21] is a microscopic many-body approach to p+p, p+A, and A+A interactions at energies ranging from SIS up to LHC. It is based on the covariant propagation of mesons and baryons. Furthermore, it includes rescattering of particles, the excitation and fragmentation of color strings, and the formation and decay of hadronic resonances. At LHC, the inclusion of hard partonic interactions in the initial stage is important and is treated via the PYTHIA [22] model.

Formation time denotes the time it takes for a hadron to be produced from a fragmenting string. A very common model to describe such a flux tube fragmentation is the Lund string model [23]. In the Lund model the formation time consists of the time it takes to produce a quark-antiquark pair and the time it takes for that pair to form a hadron. For the Lund model, both of these times are proportional to the transverse mass of the created hadron and inversely proportional to the string tension. For simplicity, UrQMD uses a constant formation time of $\tau_f = 0.8$ fm/c for hard collisions. Since HBT probes the freezeout distribution, the extracted radii are sensitive to the value of τ_f in small systems at high collision energies where the majority of particles are produced from flux tube fragmentation.

In the present study, the cascade mode of the latest version (v3.3) of UrQMD is used (for details of version 3.3. see [19, 20]). Some predictions and comparison works with data from reactions at LHC have already been pursued based on this version and showed encouraging results for the bulk properties [24, 25]. After the UrQMD simulation, all particles with their phase space distributions at their respective freeze-out time (last collisions) are put into an

analyzing program using the formalism of the well known ‘‘correlation after-burner’’ (CRAB) [26]. At last, the constructed two-pion HBT correlator (regardless of charge) in the longitudinally co-moving system (LCMS) [27, 28] without influence of residual interactions is fitted (using the χ^2 method) with a three-dimensional Gaussian form expressed as

$$C(\mathbf{q}, \mathbf{k}) = 1 + \lambda(\mathbf{k}) \exp \left[- \sum_{i,j=out,side,long} q_i q_j R_{ij}^2(\mathbf{k}) \right]. \quad (1)$$

In Eq. (1), λ represents the fraction of correlated pairs [11] and q_i is the pair relative momentum $\mathbf{q} = \mathbf{p}_1 - \mathbf{p}_2$ in the i direction, p_i being the momenta of the particles. *long* is the longitudinal direction along the beam axis, *out* is the outward direction along the transverse component of the average momentum \mathbf{k} of two particles ($\mathbf{k}_T = |\mathbf{p}_{1T} + \mathbf{p}_{2T}|/2$) and *side* is the sideward direction perpendicular to the afore mentioned directions. The effect of cross terms with $i \neq j$ on the HBT radii is found to be negligible in the present fits when the pseudorapidity cuts $|\eta| < 1.2$ and $|\eta| < 0.8$ are used for p+p and Pb+Pb cases, respectively, as in experiments, and is not discussed in this paper.

For central collisions, the HBT radii are, except for an implicit \mathbf{k}_T dependence, related to regions of homogeneity by [29]

$$R_{out}^2 = \langle (x - \beta_T t)^2 \rangle = \langle x^2 \rangle - 2 \langle \beta_T t x \rangle + \langle \beta_T^2 t^2 \rangle, \quad (2)$$

$$R_{side}^2 = \langle y^2 \rangle, \quad (3)$$

and

$$R_{long}^2 = \langle (z - \beta_L t)^2 \rangle = \langle z^2 \rangle - 2 \langle \beta_L t z \rangle + \langle \beta_L^2 t^2 \rangle, \quad (4)$$

where x , y , z and t are the spatio-temporal separation of the particles in a pair and $\beta = \mathbf{k}/k_0$. If no space-momentum correlations are present the regions of homogeneity and the source size coincide. In central collisions the relation $\langle x^2 \rangle \simeq \langle y^2 \rangle$ is satisfied. Thus R_{out}^2 and R_{side}^2 differ mainly in the last two terms of Eq. (2). The first of these two terms is dependent on the strength of the correlation of emission time and transverse emission position, while the second one is especially sensitive to the particle emission duration.

For the p+p case, the analysis is done differentially for the different event multiplicities listed in table 1. Generally, the average $dN_{ch}/d\eta$ from UrQMD is 15% smaller than the one measured by the ALICE collaboration, in the same charged multiplicity classes.

3. Results

3.1. p+p collisions at $\sqrt{s_{NN}} = 7$ TeV

In this subsection, the results on HBT radii in p+p collisions from the UrQMD model are calculated and compared to ALICE data [12]. In Fig. 1 the projections in the out, side and long directions of the 3D correlation function together with a projection of the fit for $k_T = |\mathbf{k}_T| = 0.3 - 0.4$ GeV and $N_{charged}^{|\eta| < 1.2} = 23-29$ are shown as an example. It can be seen that the calculated correlation function (shown as dots) is well described by a Gaussian fit (lines). However, oscillations of the correlation function are present at larger q . This indicates that there is a non-gaussian component in the underlying separation distribution of the pion freezeout points. Here we will not investigate this interesting question further.

The k_T dependence of the HBT radii extracted from the UrQMD freezeout distribution is presented in Fig. 2 for the $dN_{ch}/d\eta$ classes defined in table 1 in the pseudorapidity interval $|\eta| < 1.2$ in comparison to the ALICE data. The UrQMD calculations are presented for different values of the formation time τ_f ($\tau_f = 0.3$ fm/c, dashed lines; $\tau_f = 0.8$ fm/c, full lines;

Table 1. Table of the investigated multiplicity intervals. The first column shows the interval boundaries, the second column the mean charged particle multiplicity per unit of pseudorapidity ($dN_{ch}/d\eta$) from events with at least one charged particle in $|\eta| < 1.2$ from UrQMD. The third column shows the same quantity from ALICE data [12].

$N_{charged}^{ \eta <1.2}$	UrQMD $\langle dN_{ch}/d\eta \rangle_{ \eta <1.2}$	ALICE $\langle dN_{ch}/d\eta \rangle_{ \eta <1.2}$
1-11	2.52	3.2
12-16	5.74	7.4
17-22	8.01	10.4
23-29	10.72	13.6
30-36	13.65	17.1
37-44	16.74	20.2
45-57	20.94	24.2
58-149	27.57	31.1

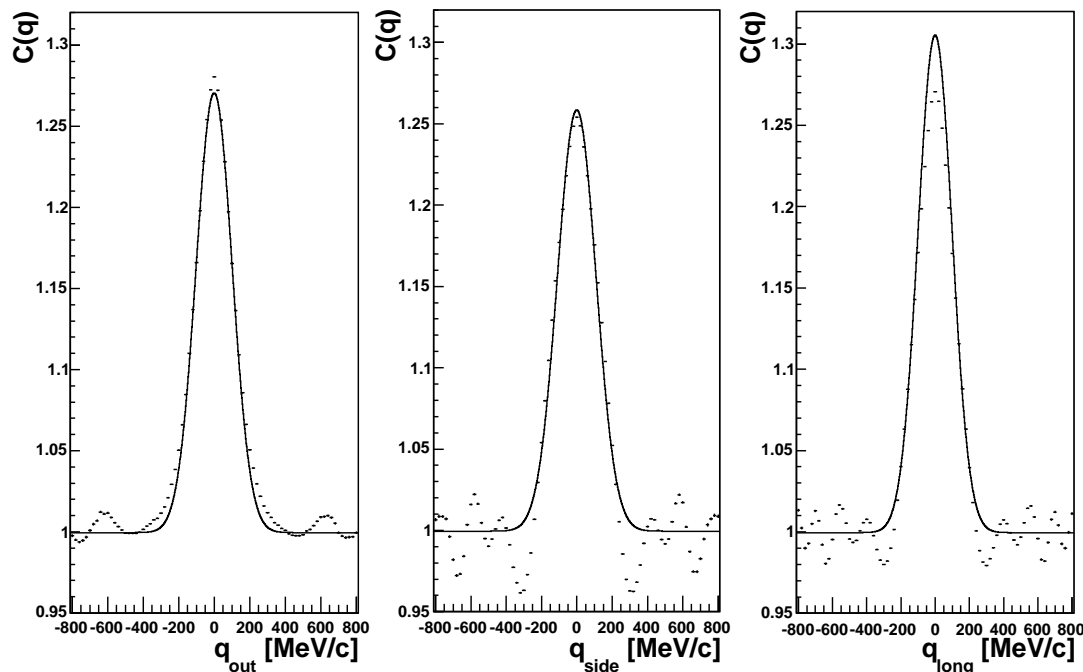


Figure 1. The dots represent projections of the three-dimensional correlation function for $k_T=0.3-0.4$ GeV and $N_{charged}^{|\eta|<1.2}=23-29$. The lines represent a χ^2 fit of Eq. (1) to the correlation function. Both the result of the fit and the correlation function are integrated over a range of $q_i = \pm 0.17$ GeV in the other directions for the purpose of projection.

$\tau_f=2$ fm/c, dotted lines). For $\tau_f=0.3$ fm/c one obtains a good description for R_{out} , while R_{side} is slightly under predicted and the values for R_{long} are in line with data from ALICE. The choice $\tau_f=0.8$ fm/c leads to a slight overestimation of R_{out} ; however, it leads to a reasonable description of R_{side} data. Also the k_T behaviour in R_{long} is much closer to the behaviour of the data. In contrast, a formation time of $\tau_f=2$ fm/c, leads to a drastic overestimation of the data for all radii. Although there are discrepancies between model and data for all values of τ_f , the

sensitivity to τ_f is much larger than those discrepancies. Therefore, the present ALICE data allows to constrain the formation time to values of $\tau_f \approx 0.3\text{-}0.8$ fm/c.

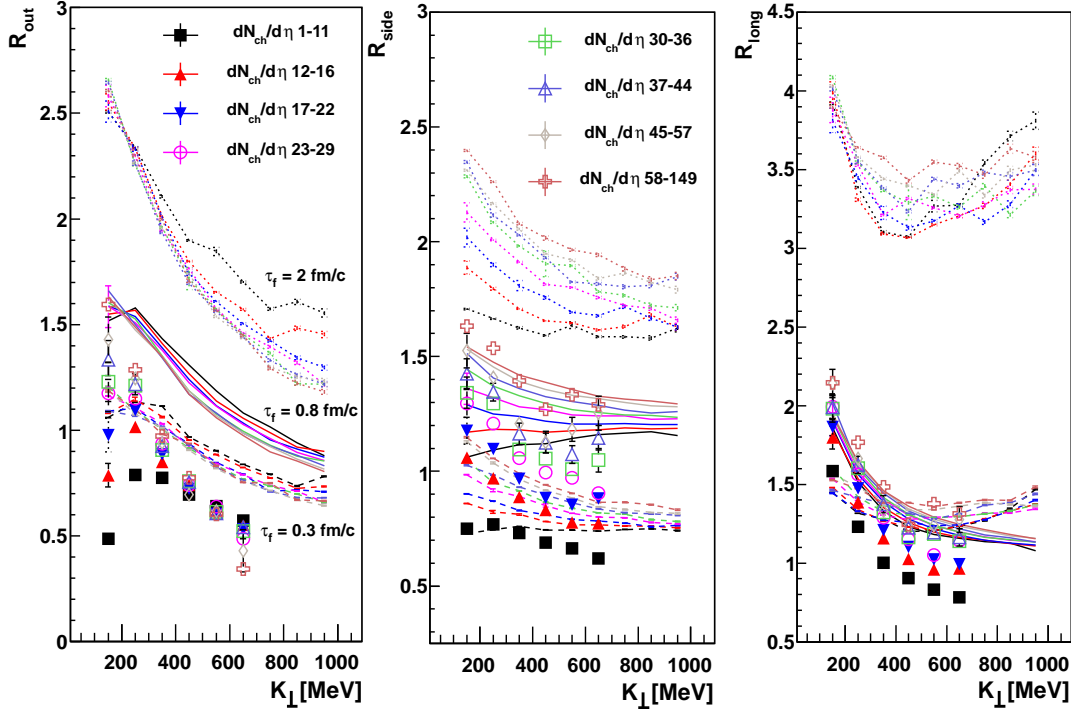


Figure 2. The lines represent HBT radii in p+p collisions at $\sqrt{s}=7$ TeV from UrQMD for different multiplicities and formation times. The various line styles refer to results for $\tau_f = 0.3$ fm/c (dashed), $\tau_f = 0.8$ fm/c (default full lines) and $\tau_f = 2$ fm/c (dotted). The colors represent the multiplicity classes as defined in table 1. The points are data from the ALICE experiment [12].

The overall shape of the radii as a function of multiplicity and k_T is also interesting. The R_{side} radii (see Fig. 2, middle) from UrQMD and in the data are flat as a function of k_T for low multiplicity events. With increasing multiplicity, the radii develop a decrease towards higher k_T . This is exactly the behavior one would expect for the development of space-momentum correlations with rising event multiplicity [16]. For R_{out} (Fig. 2, left) however, there is a k_T dependence present in all multiplicity classes. Thus, only the development of radial flow with rising particle multiplicity seems insufficient to explain the k_t dependence. Since R_{out} and R_{long} contain lifetime contributions of the source and R_{side} does not, there seem to be an additional non-trivial k_t and multiplicity dependence in the emission duration needed to explain the difference in the behavior of R_{out} , R_{side} and R_{long} . This additional correlation might be due to an additional momentum dependence in τ_f apart from the trivial Lorentz boost. This would lead to a direct effect on the emission duration, because it changes the particles production spacetime points.

3.2. Pb+Pb collisions at $\sqrt{s_{NN}} = 2.76$ TeV

Firstly, the correlation functions are also calculated in bins of the transverse momentum k_T . Fig. 3 shows the projections of the three-dimensional correlation function (dots) and of the respective fit (lines) for the k_T bin $0.2 - 0.3$ GeV/c. It is seen clearly that the correlator in

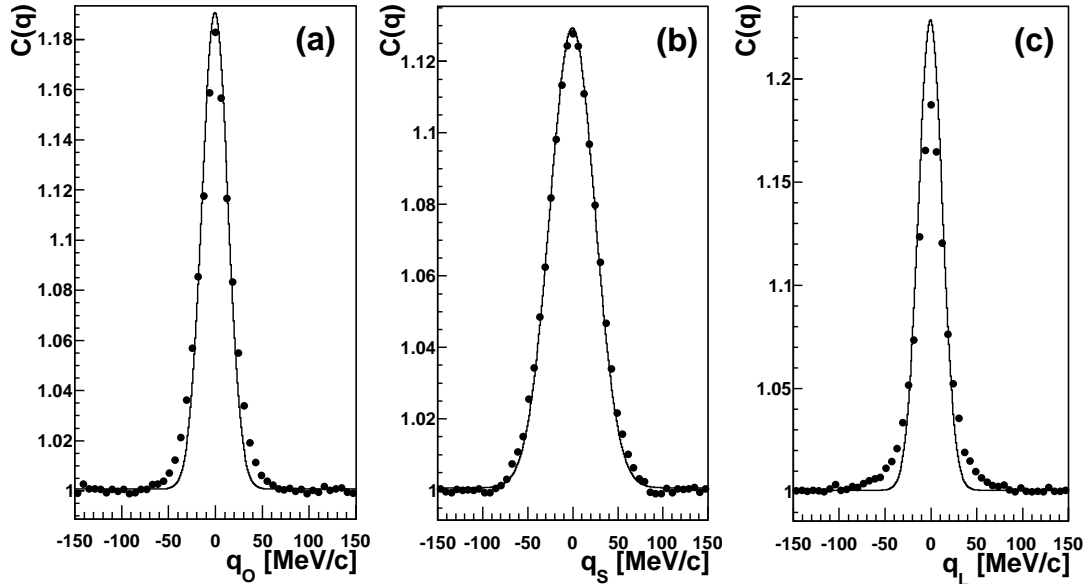


Figure 3. Projections of the three-dimensional correlation function (dots) and of the respective fit (lines) for the k_T bin $0.2 - 0.3$ GeV/c and $|\eta| < 0.8$. When projecting on one axis the other two components are restricted to the range $(-30 < q < 30)$ MeV/c.

sideward direction can be described by a Gaussian form fairly well. However, it deviates slightly from a Gaussian in the other two directions, especially in the longitudinal direction, as found and discussed in previous publications for HICs at lower energies [30]. At LHC, the fraction of excited unstable particles is much larger than at lower beam energies, therefore, the non-Gaussian effect is more pronounced in the current calculations. At RHIC energies, the non-Gaussian effect was also seen in the experimental HBT correlator, especially in the longitudinal direction [1]. Furthermore, when comparing our fitting result in Fig. 3 with that observed in experiment (in Fig. 1 of Ref. [13]), it is seen that the non-Gaussian effect is stronger in our calculations than in experiment. This might be due to the omission of all potential interactions between particles in the current cascade calculations. Support for this interpretation was found in Ref. [30], where the consideration of a mean-field potential plus Coulomb potential significantly reduced the non-Gaussian effect on correlators of pions from HICs at AGS energies. Therefore, both a dynamic treatment of the particle transport with a proper EoS for the QGP phase and the hadron phase, and further theoretical development of the fitting formalism are equally important for a more precise extraction of spatio-temporal information of the source [31].

Besides the non-Gaussian effect, the contribution of the correlation between the emission time and position to the HBT radii, especially in the outward direction, has been paid more attention in recent years since it closely relates to the stiffness of the EoS of nuclear matter especially at the early stage of the whole dynamic process [32, 33, 34]. It was found that, even in the cascade calculation, there exists a visibly positive correlation between the emission time and position [35]. And, the most important contribution to R_{out} comes from the emission duration term. It implies that both a shorter duration time and a stronger $x - t$ correlation lead to a smaller R_{out} value, which will be shown in Fig. 4 specialized for the result of HBT radii.

Fig. 4 shows the k_T dependence of the HBT radii R_{out} , R_{side} , and R_{long} , as well as the ratio R_{out}/R_{side} , extracted from the Gaussian fit to the two-pion correlators. The UrQMD cascade calculations for central Pb+Pb collisions at LHC energy $\sqrt{s_{NN}} = 2.76$ TeV (lines with crosses) and central Au+Au collisions at RHIC energy $\sqrt{s_{NN}} = 200$ GeV (lines with up-triangles) are

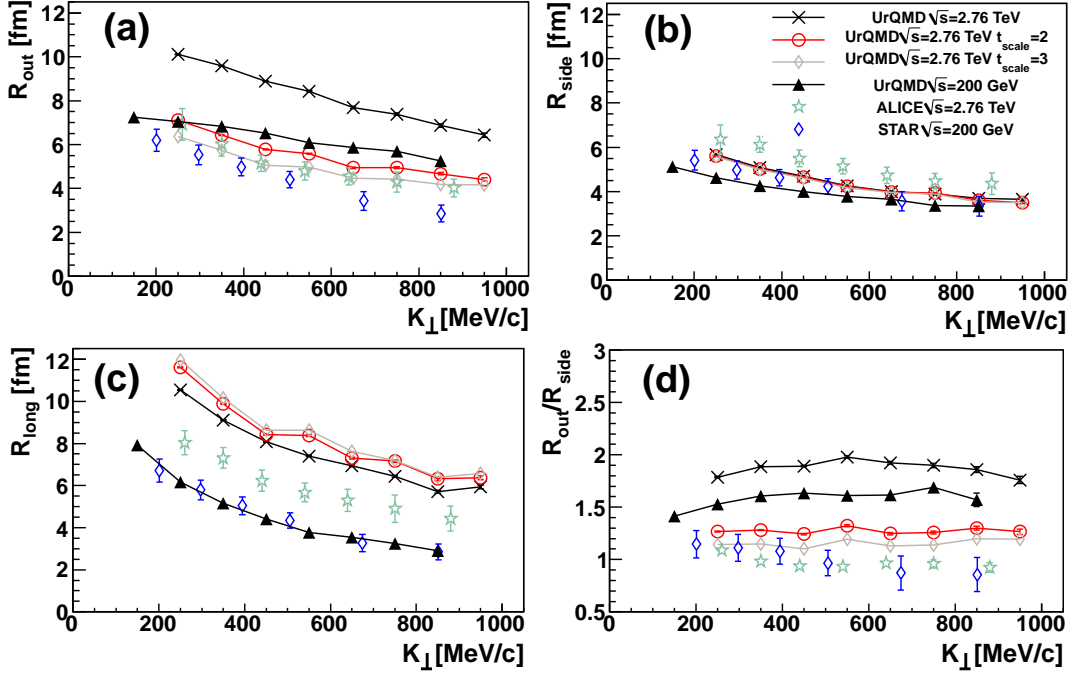


Figure 4. k_T dependence of pion HBT radii R_{out} [panel (a)], R_{side} [(b)], and R_{long} [(c)], as well as the ratio R_{out}/R_{side} [(d)], for central ($\sigma/\sigma_T < 5\%$) Pb+Pb collisions at LHC energy $\sqrt{s_{NN}} = 2.76$ TeV. For comparison, parameters for central ($\sigma/\sigma_T < 5\%$) Au+Au collisions at RHIC energy $\sqrt{s_{NN}} = 200$ GeV are also shown. Lines with up-triangles and crosses are for model calculations while scattered symbols are for experimental data of STAR/RHIC and ALICE/LHC collaborations taken from [1, 13]. Lines with circles and diamonds show results with an artificially decreased emission duration by a factor of $t_{scale} = 2$ and 3, separately, in the analysis of correlation function.

compared to corresponding experimental data by ALICE/LHC (open stars) and STAR/RHIC (open diamonds). A strong decrease of the three HBT-radii with k_T is seen both in experiments and in the UrQMD calculations for HICs. This implies a substantial expansion of the source and is qualitatively captured by the UrQMD dynamics. Following experimental results, the calculated HBT radii for Pb+Pb at LHC are found to be larger than those for Au+Au at RHIC. The largest increase exists in the longitudinal direction, which is also seen by the experiments. Although the comparison of the calculated HBT radii R_{long} and R_{side} with corresponding data at RHIC is fairly well, it gets worse when going to the higher LHC energy. At LHC the calculated R_{side} values at all k_T are found to be slightly smaller than data, while R_{long} and R_{out} values are larger than data. Together with large calculated R_{out} , the emission time related quantity R_{out}/R_{side} is found to be markedly larger than the data.

From Eq. (2) it is clear that the value of R_{out} is strongly dependent on the emission duration of the particles. To further investigate the contribution of the emission duration to the HBT radii, we artificially decrease it by rescaling the relative time t to the “effective source center time” \bar{t} ($= \langle t_i \rangle$) by $t = t_i - \bar{t} \rightarrow t' = (t_i - \bar{t})/t_{scale}$ in the calculation of the correlation function at LHC energies. This effectively changes Eq. (2) to

$$R_{out}^2 = \langle (x - \beta_T t')^2 \rangle = \langle x^2 \rangle - 2 \frac{\langle \beta_T t x \rangle}{t_{scale}} + \frac{\langle \beta_T^2 t^2 \rangle}{t_{scale}^2}. \quad (5)$$

The results for this calculation are presented as lines with circles ($t_{scale} = 2$) and with diamonds

($t_{scale} = 3$) in Fig. 4. The artificially decreased emission duration leads to smaller R_{out} values in all k_T bins but leaves R_{side} unchanged, as expected. Overall it results in an improved agreement with the data of R_{out}/R_{side} ratio. From Fig. 4 it is also found that R_{long} is overestimated at LHC. Since R_{long} is mainly related to the lifetime of the source, it implies that this lifetime is also overestimated by UrQMD. Other calculations in [13, 36] show that UrQMD overestimates the source lifetime by a factor of $\sim 2 - 3$ when compared to LHC data. The overestimation of both R_{out} and R_{long} can be attributed to the known fact that the pressure in the early stage is not strong enough in the cascade model calculations. A higher pressure would lead to a more explosive expansion, a stronger phase-space correlation, and a faster decoupling of the system, thus leading to smaller regions of homogeneity. For more discussion we refer the reader to [31, 33]. With the improved integrated Boltzmann + hydrodynamics hybrid approach [20, 25, 37, 38], where various EoS of nuclear matter during the hydrodynamic evolution may be treated consistently and a decoupling supplemented by realistic three-dimensional hypersurfaces we hope to get a satisfactory solution in the near future.

4. Summary

To summarize, two-pion HBT correlations for p+p and central Pb+Pb collisions at the LHC energies are investigated with the UrQMD model combined with a correlation afterburner CRAB. The transverse momentum dependence of the Pratt-Bertsch HBT radii R_{long} , R_{out} , and R_{side} is extracted from a three-dimensional Gaussian fit to the correlator in the LCMS system. It is seen that the correlator in sideward direction can be described by a Gaussian form fairly well while non-Gaussian effect is seen in both longitudinal and outward directions.

In the p+p collisions, we have shown that the data provides rather direct access to the particle formation times in the flux tube fragmentation. The sensitivity to τ_f is large enough compared to the model uncertainties to find that a value $\tau_f = 0.3 - 0.8$ fm/c is strongly favored compared to larger values for τ_f . Values of $\tau_f \geq 2$ fm/c can be ruled out from the present analysis.

In the Pb+Pb case, both the transverse momentum k_T dependence and the beam energy (from RHIC to LHC) dependence of the HBT radii R_{out} , R_{side} , and R_{long} exhibit qualitatively the same behavior as found in the experiments. However, the calculated R_{out}/R_{side} ratios at all k_T bins are found to be larger than in the data, both at RHIC & LHC. We traced this finding back to the explosive dynamics of the fireball at LHC which results in both a shorter emission duration and a stronger time-space correlation than modeled here.

Acknowledgments

This work was supported by the Helmholtz International Center for FAIR within the framework of the LOEWE program launched by the State of Hesse, GSI, and BMBF. Q.L. thanks the financial support by the NNSF (Nos. 10905021, 10979023), the Zhejiang Provincial NSF (No. Y6090210), and the Qian-Jiang Talents Project of Zhejiang Province (No. 2010R10102) of China.

References

- [1] Adams J *et al.* [STAR Collaboration] 2005 *Phys. Rev. C* **71** 044906
- [2] Lisa M A *et al.* [E895 Collaboration] 2000 *Phys. Rev. Lett.* **84** 2798
- [3] Alt C *et al.* [NA49 Collaboration] 2008 *Phys. Rev. C* **77** 064908
- [4] Afanasiev S V *et al.* [NA49 Collaboration] 2002 *Phys. Rev. C* **66** 054902
- [5] Adamová D *et al.* [CERES Collaboration] 2003 *Nucl. Phys. A* **714** 124
- [6] Abelev B I *et al.* [STAR Collaboration] 2009 *Phys. Rev. C* **80** 024905
- [7] Back B B *et al.* [PHOBOS Collaboration] 2006 *Phys. Rev. C* **73** 031901
- [8] Back B B *et al.* [PHOBOS Collaboration] 2006 *Phys. Rev. C* **73** 021901
- [9] Back B B *et al.* [PHOBOS Collaboration] 2003 *Phys. Rev. Lett.* **91** 052303
- [10] Abelev B I *et al.* [STAR Collaboration] 2009 *Phys. Rev. C* **79** 034909

- [11] Pratt S, Soltz R and Wiedemann U 2005 *Ann. Rev. Nucl. Part. Sci.* **55** 357
- [12] Aamodt K *et al.* [ALICE Collaboration] 2011 *Phys. Rev. D* **84** 112004
- [13] Aamodt K *et al.* [ALICE Collaboration] 2011 *Phys. Lett. B* **696** 328
- [14] Karpenko Y A and Sinyukov Y M 2011 *J. Phys. G* **38** 124059
- [15] Humanic T J 2011 *arXiv:1011.0378 [nucl-th]*
- [16] Werner K, Mikhailov K, Karpenko I and Pierog T 2011 *arXiv:1104.2405 [hep-ph]*
- [17] Bass S A *et al.* 1998 *Prog. Part. Nucl. Phys.* **41** 255
- [18] Bleicher M *et al.* 1999 *J. Phys. G* **25** 1859
- [19] Petersen H, Bleicher M, Bass S A and Stocker H 2008 *arXiv:0805.0567 [hep-ph]*
- [20] Petersen H, Steinheimer J, Burau G, Bleicher M and Stocker H 2008 *Phys. Rev. C* **78** 044901
- [21] Li Q F, Shen C W, Guo C C, Wang Y J, Li Z X, Lukasik J and Trautmann W 2011 *Phys. Rev. C* **83** 044617
- [22] Sjostrand T, Mrenna S and Skands P Z 2006 *JHEP* **0605** 026
- [23] Andersson B, Gustafson G, Ingelman G and Sjostrand T 1983 *Phys. Rept.* **97** 31
- [24] Mitrovski M, Schuster T, Graf G, Petersen H and Bleicher M 2009 *Phys. Rev. C* **79** 044901
- [25] Petersen H 2011 *Phys. Rev. C* **84** 034912
- [26] Pratt S *et al.* 1994 *Nucl. Phys. A* **566** 103C
- [27] Pratt S 1986 *Phys. Rev. D* **33** 1314
- [28] Bertsch G, Gong M and Tohyama M 1988 *Phys. Rev. C* **37** 1896
- [29] Wiedemann U A and Heinz U W 1999 *Phys. Rept.* **319** 145
- [30] Li Q and Bleicher M 2009 *J. Phys. G* **36** 015111
- [31] Pratt S 2009 *Acta Phys. Polon.* **B40** 1249
- [32] Lin Z W, Ko C M and Pal S 2002 *Phys. Rev. Lett.* **89** 152301
- [33] Li Q, Bleicher M and Stocker H 2008 *Phys. Lett. B* **659** 525
- [34] Li Q, Steinheimer J, Petersen H, Bleicher M and Stocker H 2009 *Phys. Lett. B* **674** 111
- [35] Li Q, Graef G and Bleicher M 2012 *Phys. Rev. C* **85** 034908
- [36] Graef G, Bleicher M and Li Q 2012 *Phys. Rev. C* **85** 044901
- [37] Steinheimer J, Schramm S and Stocker H 2011 *J. Phys. G* **38** 035001
- [38] Steinheimer J and Bleicher M 2011 *Phys. Rev. C* **84** 024905